Supplementary Figures

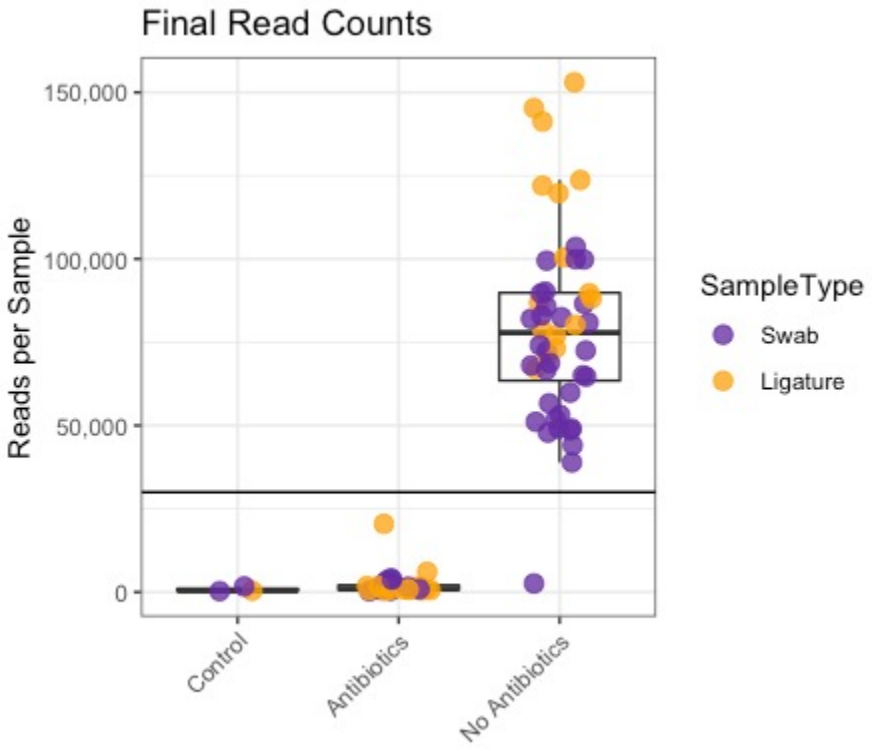

Figure S1. Final read counts from antibiotic-treated and untreated mice. To determine the influence of the microbiome on ligature-associated periodontitis, some mice were given an antibiotic cocktail in their drinking water (1 mg/mL each of ampicillin, cefoperazone sodium salt, and clindamycin hydrochloride) starting 2 weeks before ligature placement and continued until the conclusion of the experiment (Antibiotic-treated). Control mice received drinking water without antibiotics (No antibiotics). Uninoculated swabs served as a control blank. Efficacy of the antibiotic treatment was confirmed by sampling the microbiome from oral swabs and ligatures and evaluating OTU counts generated as described in the Methods. Due to low confidence in samples with too few reads, a cutoff of 30,000 reads was implemented. All controls and antibiotic-treated samples were, therefore, excluded from downstream analyses, as well as one ligated S100A9$^{-/-}$ swab, sample 804.

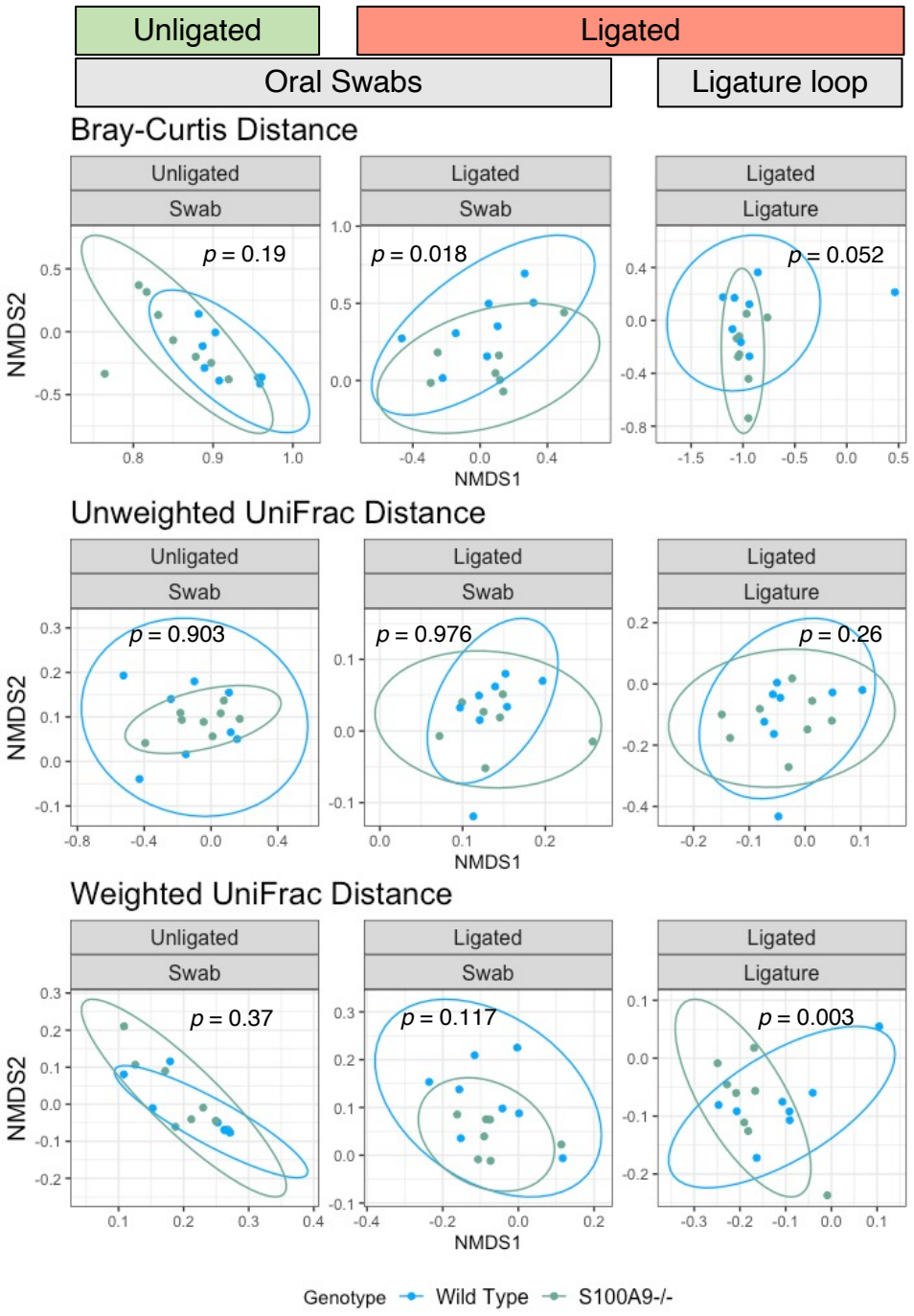

Figure S2. Microbiome dissimilarity between ligated and unligated sites/samples from WT and S100A8/A9^{null} mice. Beta diversity was evaluated with Bray-Curtis distance and both unweighted and weighted UniFrac distances to compare diversity between samples. Distances were visualized using non-metric multidimensional scaling (NMDS), and genotype group differences were evaluated using a PERMANOVA test as shown on corresponding plots.

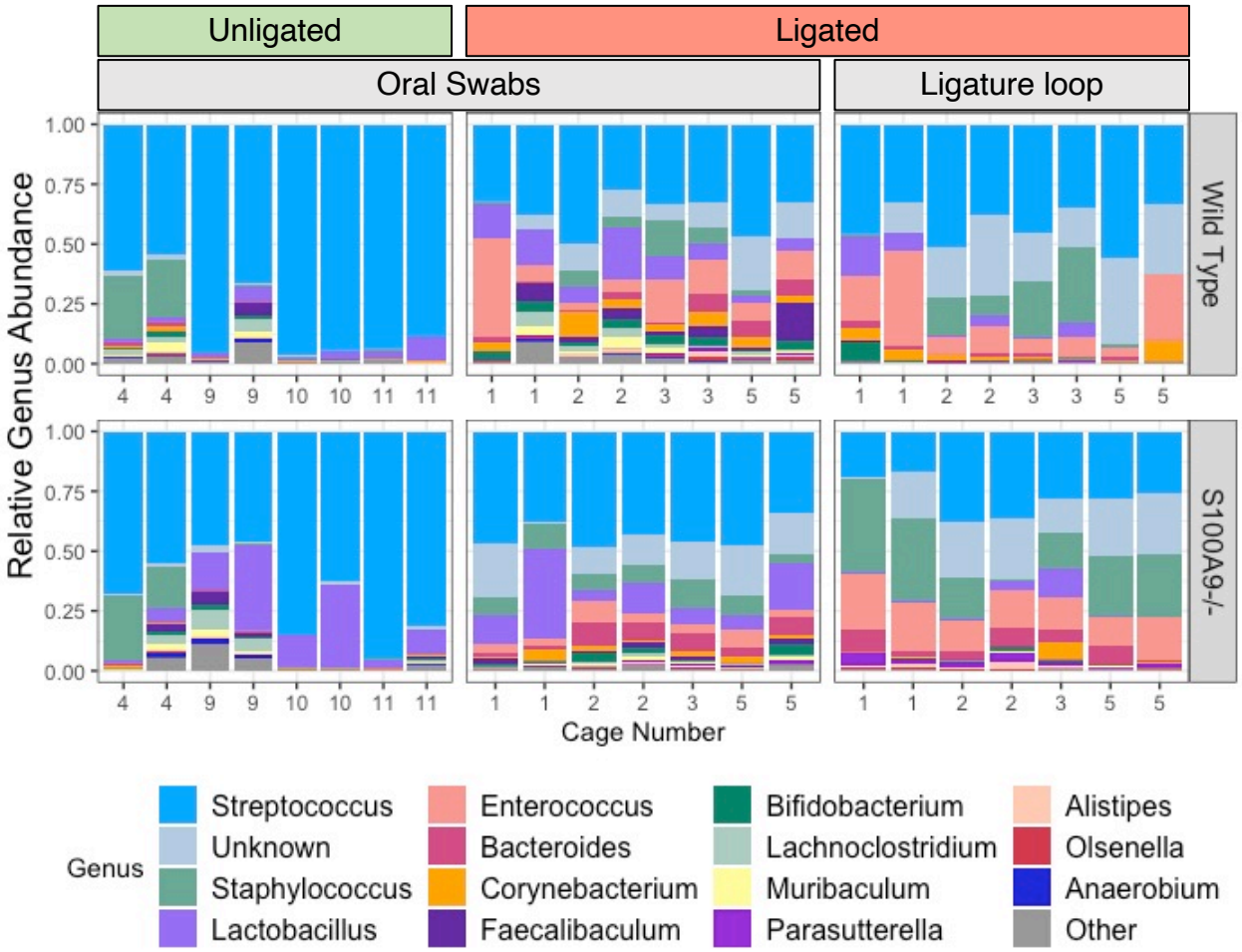

Figure S3. Microbial relative abundances differ in S100A9$^{-/-}$ than WT mice at sites of inflammation (5 days). Each sample, grouped by ligation treatment, sample type, and caging, is displayed as a stacked bar representing the relative abundance of genera in the sample as described in the Methods. The legend provides the name of the genus represented by each color in order; the "Unknown" category is the combination of all genera which were identified as OTUs but could not be assigned a taxonomic name. "Other" is the combination of known taxonomies that were too small in relative abundance to be included as individual colors in this figure. Note there is one fewer swab and ligature in the S100A9$^{-/-}$ group because a sample was excluded due to low read counts.

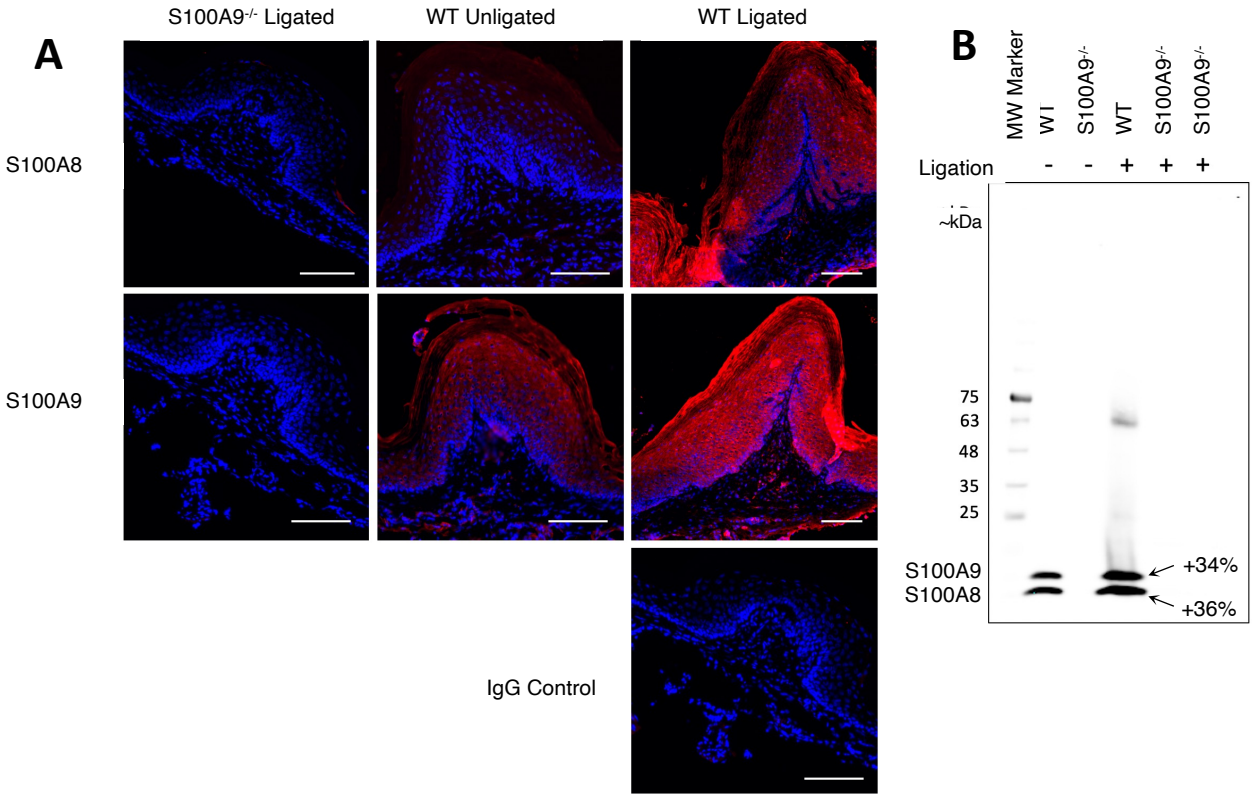

Figure S4. Ligature-induced periodontitis upregulates expression of S100A8 and S100A9 in oral gingival tissues. Five days after ligature placement in S100A8/A9$^{-/-}$ and WT mice (see Materials and Methods), gingiva was harvested adjacent to the ligated tooth and the contralateral unligated side (control). **(A) Immunohistochemical staining of tissue sections for S100A8 and S100A9.** Reagents included DAPI (blue), goat anti-mouse S100A8 polyclonal antibody, goat anti-mouse S100A9 polyclonal antibody, polyclonal goat IgG (control), donkey anti-goat IgG (H+L) secondary antibody, and Alexa Fluor 647 (red) as described in the Methods. The IgG control includes secondary antibody. Representative images of sagittal sections through the gingiva (see Figure S2A) are shown. White bars = 100 µm. **(B) Western Blot confirmation of calprotectin protein in the tissues.** Protein was extracted from the gingiva of ligated and unligated WT mice and analyzed using Western blotting as described in the Methods. Arrows indicate an increase in band density compared to WT without ligation. No expression of S100A8 or S100A9 protein was observed in S100A9$^{-/-}$ mice.

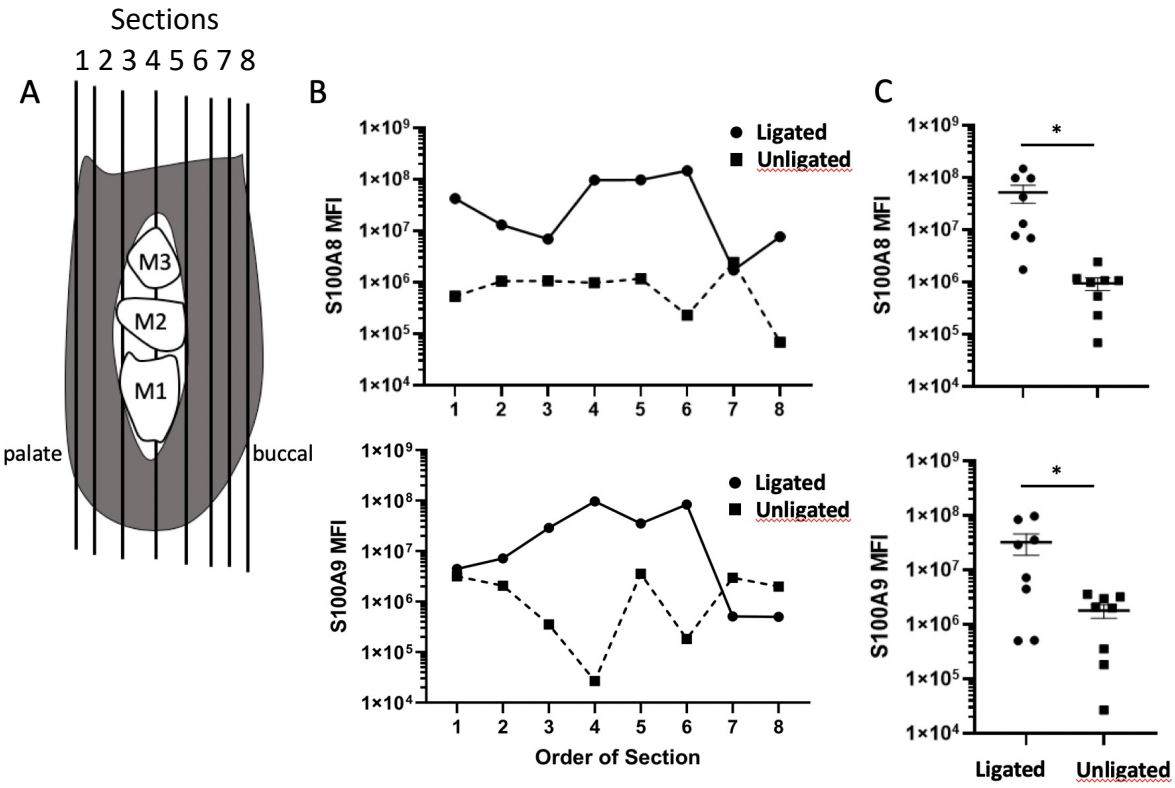

Figure S5. S100A8 and S100A9 expression increases in the gingiva adjacent to the ligated tooth. (A) Representative birds-eye view of sagittal sectioning starting on the buccal side of the maxillary tissue. M1, M2, and M3 identify the first, second, and third molar teeth, respectively. **(B)** Expression of S100A8 (upper panel) and S100A9 (lower) in sequential sections from ligated control and unligated gingiva from the contralateral side of the maxilla. Expression of S100A8 and S100A9 increased in sections immediately proximal to the ligated tooth (sections 3-6) as quantified by mean fluorescence intensity (MFI) as reported in the Methods. **(C)** S100A8 and S100A9 levels in ligated sections were significantly greater than unligated contralateral controls. (*$p<0.05$)

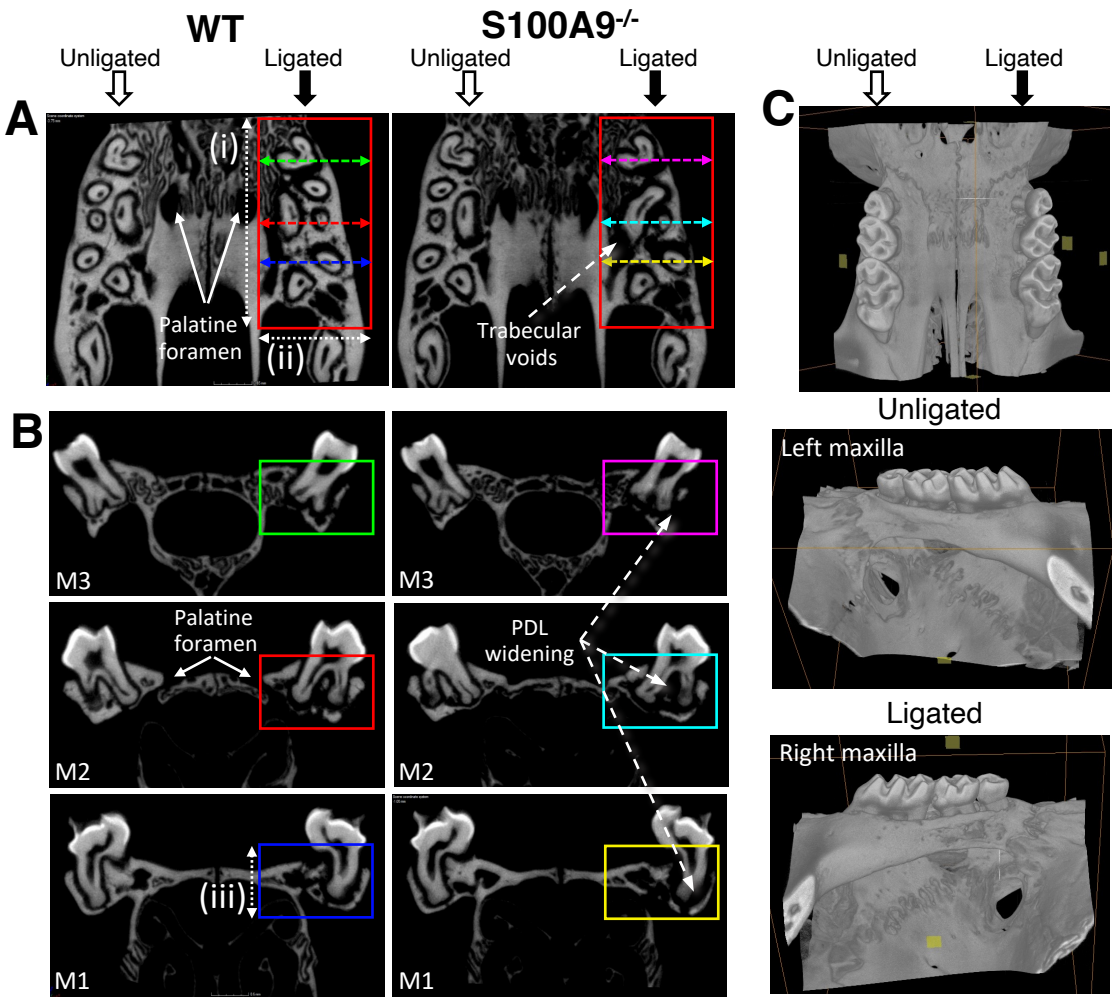
WT
S100A9-/-
Unligated
Ligated
Unligated
Ligated
A
(i)
(ii)
Palatine foramen
Trabecular voids
C
Unligated
Ligated
B
M3
M3
Palatine foramen
PDL widening
M2
M2
(iii)
M1
M1
Unligated
Left maxilla
Ligated
Right maxilla

Figure S6. Representative images of reconstructed micro-computed tomography of ligated mouse jaws. Day 5 ligated WT and S100A9$^{-/-}$ maxillae were harvested, scanned with micro-CT and reconstructed using CT Pro 3. Volumes were loaded into VG Studio MAX to generate BMP datasets then imported into Data Viewer as described in the Methods. After reconstruction, datasets were viewed slice-by-slice or as three orthogonal projections. **(A)** Horizontal sections through the maxillae displaying the unligated (open arrow) and ligated (filled arrow) sides. The (i) mesio-distal and (ii) bucco-palatal boundaries of the volume of interest (VOI) (red rectangle) are also shown. The colored dotted arrows correspond to the orthogonal sections displayed in the frontal plane in B. **(B)** Frontal sections through the maxilla displaying the (iii) apico-coronal boundaries of the VOI. Trabecular voids are seen in the alveolar bone and periodontal ligament space (white segmented arrows) surrounding the roots of the ligated second molar (M2) teeth and the adjacent first and third molars (M1 and M3 respectively). Voids were not apparent on the unligated contralateral sides (open arrows). Voids appear larger in S100A9$^{-/-}$ than WT mice. **(C)** When examined in 3D, greater bone loss was associated with the ligature than the unligated contralateral side as seen in a representative WT mouse.

Table S1. Mean relative abundances of the top 10 genera overall in ligated and unligated sites/samples from WT and S100A9$^{-/-}$ mice.*

Mean Relative Abundance						
Genus	Unligated Swabs		Ligated Swabs		Ligature loops	
	Wild Type	S100A9$^{-/-}$	Wild Type	S100A9$^{-/-}$	Wild Type	S100A9$^{-/-}$
Streptococcus	0.81	0.68	0.37	0.43	0.42	0.27
Staphylococcus	0.07	0.06	0.04	0.08	0.10	0.23
Lactobacillus	0.03	0.15	0.10	0.14	0.04	0.03
Enterococcus	0.001	0.002	0.14	0.05	0.15	0.16
Bacteroides	0.003	0.003	0.04	0.06	0.01	0.05
Corynebacterium	0.01	0.004	0.04	0.02	0.03	0.01
Faecalibaculum	0.01	0.01	0.05	0.01	0.001	0.002
Bifidobacterium	0.01	0.01	0.03	0.02	0.01	0.004
Lachnoclostridium	0.01	0.02	0.02	0.006	0.0002	0.0001
Muribaculum	0.01	0.01	0.02	0.007	0.0006	0.001

* Data was calculated are reported in the Methods. After ligation, the Streptococcus genus was clearly less dominant in both wild type and S100A9$^{-/-}$ mice in the swab and ligature samples. The change in alpha diversity with ligation seen in Figure 1 is represented here by a seemingly more even distribution of relative abundance across genera.